J. Plasma Physics (2014), *vol.* 80, *part* 2, *pp.* 225–234. © Cambridge University Press 2013
doi:10.1017/S0022377813001220

Wakefield effects on three-dimensional dust-lattice modes

B. Farokhi† and A. Hameditabar

Department of Physics, Arak University, Arak, Iran
(b-farokhi@araku.ac.ir)

(Received 18 March 2013; revised 27 August 2013; accepted 1 October 2013;
first published online 13 December 2013)

Dispersion relations of dust-lattice waves in three-dimensional body-centered cubic (bcc) and face-centered cubic (fcc) dusty plasma crystals are derived taking into account particle–wake interactions. Results show that resonance coupling between the longitudinal and out-of-plane transverse wave modes set in if the vertical confinement is below a certain critical value. The imaginary part of the wave frequency shows that the hybrid mode cannot propagate in the crystal.

1. Introduction

In the last decade, dusty plasma crystals have been extensively studied both theoretically and experimentally. Several experiments performed in different laboratories and simulations have demonstrated the formation of dust crystals. Dust lattices are often found near the sheath region where the electrostatic force balances the gravitational and other forces. In many laboratory experiments, micron-sized grains acquire so significant charge Q and small separation a that the ratio of the average electrostatic potential energy to the thermal energy $k_B T_d$, i.e. $\Gamma = Q^2/4\pi\varepsilon_0 a k_B T_d$, exceeds 170, dust particles arranged in ordered crystalline structures (Ikezi 1764). The study of plasma crystal provides a useful tool for investigating lattice defects, dislocations, interaction with waves, resonances in solid states, etc. Most Coulomb crystal structures that have been reported to be observed in dusty plasmas are two-dimensional (2D) hexagonal structures (Thomas et al. 1994; Hamaguchi et al. 1997a; Ivlev and Morfill 2001; Vaulina et al. 2002; Bonitz et al. 2010), and some are 3D hexagonal structures such as body-centered cubic (bcc) or face-centered cubic (fcc) (Chu and Lin 1994; Pieper et al. 1996; Hayashi 1999; Zuzic et al. 2000; Klumov and Morfill 2008). The domain of Γ and lattice parameter, $\kappa = a/\lambda_D$, are important for crystallizing into 3D bcc and fcc configurations (Hamaguchi et al. 1997b), thus we chose $\kappa = 1.2$ for bcc and $\kappa = 2.5$ for fcc lattice.

The external electric field, such as that found in experimental complex plasmas, reshape interaction potential around dust particles. Dust particles in laboratory typically levitate in the sheath region above a powered lower electrode within a radio-frequency (rf) discharge plasma. In this region, the electric field points toward the lower electrode, creating an ion flow in this direction. The corresponding potential field around the dust is commonly referred to as the wakefield. The wakefield has been studied extensively both theoretically and experimentally due to its importance to the overall structural development and dynamics of complex plasmas (Schweigert

† Email address for correspondence: b-farokhi@araku.ac.ir

https://doi.org/10.1017/S0022377813001220 Published online by Cambridge University Press

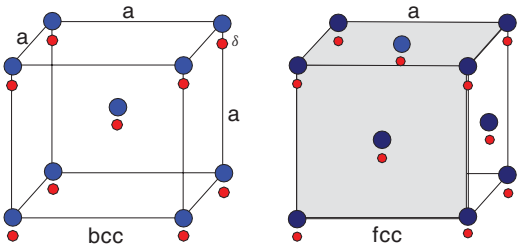


FIGURE 1. (Colour online) bcc and fcc structures of dust lattices.

et al. 1996; Morfill et al. 1997; Ignatov 2003). Experiments have found that the wakefield is attractive and non-reciprocal, which may be the cause for the vertically aligned structure of resulting plasma crystals. In the sheath region, the screening cloud around a charged grain is asymmetric and it makes the interaction between the particles very peculiar. The wakefield idea has been experimentally verified in a vertical chain in which a lower dust particle is attracted toward the upper particle in a plasma with ion flow (Morfill et al. 1997), and then theoretical study re-examines the modification of the Debye–Huckel repulsive and wakefield attractive potentials in an unmagnetized dusty plasma, including ion flow in the sheath region (Ignatov 2003). The attractive forces of these ion clouds in the lower layer particles are shown to lead to vertical alignments in theoretical studies effect of ion flow, modeled as the excess positive charge q of the wake (along the vertical axis), located at some distance δ beneath the particle (Schweigert et al. 1996). Zhanov et al. (2009) carried out theoretical investigation of (DL) wave mode coupling in 2D plasma crystals due to particle–wake interactions. They studied the instability due to resonance coupling between out-of-plane mode and in-plane mode with longitudinal polarization.

The linear modes in simple cubic, bcc, and fcc lattices, without the wake-charge effects, are studied theoretically in Wang et al. (2006); Yang et al. (2009); Farokhi and Hameditabar (2012); and Yang and Wang (2012). In experiments, plasma crystals are confined by an external electric field not only in the vertical direction but also in the horizontal direction by electrodes on the sides. Thus, the boundary effects and the ion streaming (therefore the wake) in horizontal and vertical directions are important. We have assumed that the system has a very large extension in the horizontal direction and thus the boundary effect can be ignored in the region away from the sides. Simulations indicate the type of confinement potential. A detailed analysis of confinement potential by molecular dynamics simulation is investigated on the 3D structure of dusty plasma (Klumov and Morfill 2009).

In this paper, the linear modes in the bcc and fcc dust-lattice configurations are studied. The effects of wake-charge on the dispersion relation, coupling, and instability are investigated.

2. Basic equations

Consider a 3D dust crystal with lattice spacing, a consisting of negative charge dust grains, Q and mass, M, modeled as point charges. The excess positive charge q of the wake (along the vertical axis), located at some distance, δ beneath the particle is used. Vertically, the particles are confined in a parabolic potential well, $U_{\mathrm{Conf}} = M\Omega_{\mathrm{Conf}}^2 z^2/2$. The system has a very large extension in the horizontal direction, and thus the boundary effect can be ignored in the middle of the crystal. Figure 1 shows the bcc and fcc dust-lattice configurations.

https://doi.org/10.1017/S0022377813001220 Published online by Cambridge University Press

Consider the ith particle position, $\mathbf{r_i} = \mathbf{r_{0i}} + \mathbf{d_i}$ (r_{0i} is the equilibrium position vector of the particle and $\mathbf{d} = (\mathbf{u}, \mathbf{v}, \mathbf{w})$ indicates displacement from equilibrium). Here we denoted the relative distance between particles by $r = r_i - r_j$ so that the distance from one particle to the wake of another one is $\mathbf{r} - \delta\hat{\mathbf{z}}$.

We may expand the repulsive Debye–Huckel interaction potential energy and the attractive potential energy between one particle and the wake of another one around equilibrium at $r = r_0$and keep until the linear term in force,

$$U(r) = \frac{Q^2}{4\pi\varepsilon_0}\frac{\exp(-|\mathbf{r}|/\lambda_D)}{|\mathbf{r}|} - \frac{qQ}{4\pi\varepsilon_0}\frac{\exp(-|\mathbf{r}-\delta\hat{\mathbf{z}}|/\lambda_D)}{|r-\delta\hat{\mathbf{z}}|}, \tag{1}$$

$$U(r) = U(r_0) + (r-r_0)\left.\frac{\partial U}{\partial r}\right|_{r=r_0} + \frac{1}{2}(r-r_0)^2\left.\frac{\partial^2 U}{\partial r^2}\right|_{r=r_0} + \cdots \tag{2}$$

The electrostatic binary interaction force exerted on dust grains is $F = -\partial U/\partial r$. For the analysis of dust-lattice waves, we employ the equation of motion for individual particles,

$$M\ddot{d} + M\nu\dot{d} = -M\Omega_{\mathrm{Conf}}^2 w + \sum_i \left[\left(-\frac{\partial U}{\partial r}\right)\Big|_{r=r_0} + \left(-\frac{\partial^2 U}{\partial r^2}\right)\Big|_{r=r_0}(r_i - r_0)\right]\nabla(r_i - r_0), \tag{3}$$

where ν is the damping friction. For the waves propagating in the x–y plane, letting $d_i \propto \exp(-i\omega t + ik.r_{0i})$ into (3) and neglecting nonlinear terms, we thus obtain the dispersion relation of dust-lattice modes by

$$\det[\omega(\omega + i\nu)\mathbf{I} - \mathbf{K}] = 0. \tag{4a}$$

$$\mathbf{K} = \begin{pmatrix} \alpha_1 + \alpha_2 & -\gamma & i\sigma_x \\ -\gamma & \alpha_1 + \alpha_3 & i\sigma_y \\ -i\sigma_x & -i\sigma_y & \alpha_1 + \Omega_{\mathrm{Conf}}^2 \end{pmatrix}, \tag{4b}$$

where $\mathbf{I}$ is the unit matrix. The frequency is normalized by $\omega_0 = \sqrt{Q^2/4\pi\varepsilon_0 Ma^3}$. Obviously, the elements of matrix $\mathbf{K}$ are different for bcc and fcc configurations.

2.1. *Dispersion relations of the bcc configuration*

The matrix elements in the bcc configuration are

$$\alpha_1 = [16\sqrt{3}(1-\tilde{q})\kappa^2/9]\exp(-\sqrt{3}\kappa/2)\left[\sin^2\left(\frac{k_x+k_y}{4}a\right) + \sin^2\left(\frac{k_x-k_y}{4}a\right)\right], \tag{5a}$$

$$\alpha_2 = (1-\tilde{q})\exp(-\kappa)\left[(8+8\kappa+4\kappa^2)\sin^2\left(\frac{k_x}{2}a\right) - (1+\kappa)\sin^2\left(\frac{k_y}{2}a\right)\right], \tag{5b}$$

$$\alpha_3 = (1-\tilde{q})\exp(-\kappa)\left[(8+8\kappa+4\kappa^2)\sin^2\left(\frac{k_y}{2}a\right) - (1+\kappa)\sin^2\left(\frac{k_x}{2}a\right)\right], \tag{5c}$$

$$\gamma = (1-\tilde{q})\Omega_1\left[\sin^2\left(\frac{k_x+k_y}{4}a\right) - \sin^2\left(\frac{k_x-k_y}{4}a\right)\right], \tag{5d}$$

$$\sigma_x = \tilde{q}\tilde{\delta}\Omega_1\left[\sin\left(\frac{k_x+k_y}{2}a\right) + \sin\left(\frac{k_x-k_y}{2}a\right)\right] + \tilde{q}\tilde{\delta}\Omega_2\sin(k_x a), \tag{5e}$$

https://doi.org/10.1017/S0022377813001220 Published online by Cambridge University Press

$$\sigma_y = \tilde{q}\tilde{\delta}\Omega_1 \left[\sin\left(\frac{k_x + k_y}{4}a\right) - \sin\left(\frac{k_x - k_y}{4}a\right)\right] + \tilde{q}\tilde{\delta}\Omega_2 \sin(k_y a), \tag{5f}$$

$$\Omega_1 = [16(4\sqrt{3} + 6\kappa + \sqrt{3}\kappa^2)/9]\exp(-\sqrt{3}\kappa/2), \tag{5g}$$

$$\Omega_2 = (6 + 6\kappa + 2\kappa^2)\exp(-\kappa), \tag{5h}$$

where $\tilde{q} = q/Q$ and $\tilde{\delta} = \delta/a$ are the normalized wake-charge and wake-distance, respectively. The lattice constant $\kappa = a/\lambda_D$ shows the range of screening. For deriving (5), the condition $\tilde{\delta}^2 \ll 1$ is used.

Now Let us first point out the dust-lattice modes described by (4) for $\tilde{q} = 0$. Equation (5) shows that coefficients σ_x and σ_y depend on wake-charge $\tilde{q}$ and $\sigma_x = \sigma_y = 0$. By adopting the notation $\Omega \equiv \sqrt{\omega(\omega + i\nu)} \cong \omega + i\nu/2$ for eigenvalues, we write the dispersion relation in the following form:

$$(\Omega^2 - \Omega_+^2)(\Omega^2 - \Omega_-^2)\left(\Omega^2 - \Omega_V^2\right) = 0, \tag{6}$$

where $\Omega_\pm^2 = [(2\alpha_1 + \alpha_2 + \alpha_3) \pm \sqrt{(\alpha_2 - \alpha_3)^2 + 4\gamma^2}]/2$ is a pair of in-plane (horizontal) frequencies and $\Omega_V^2 = \Omega_{\text{Conf}}^2 + \alpha_1$ is the optical out-of-plane frequency. For $\tilde{q} \neq 0$, the dispersion relation (4) is governed by

$$\begin{aligned}(\Omega^2 - \Omega_+^2)(\Omega^2 - \Omega_-^2)(\Omega^2 - \Omega_V^2) + \sigma_x^2(\Omega^2 - \alpha_1 - \alpha_3) \\ + \sigma_y^2(\Omega^2 - \alpha_1 - \alpha_2) + 2\gamma\sigma_x\sigma_y = 0.\end{aligned} \tag{7}$$

Due to $\sigma_{x,y} \sim \tilde{q}\tilde{\delta} \ll 1$, all terms of coupling in dispersion relations are much smaller than any of the mode frequencies $\Omega_\pm$, Ω_V. At small wavenumber ka, the out-of-plane mode is larger than either of the in-plane modes, but the longitudinal mode of in-plane vibration can be compared with the out-of-plane mode at larger ka, where they may cross. It is obvious that the coupling can only be triggered when the confinement frequency Ω_{Conf} is below a critical value, which corresponds to the junction between the modes.

In a special case, when the wave propagates in (1,0,0) direction ($k_x = k, k_y = 0$), the dispersion relation of modes reduces to

$$\omega_1 = \sqrt{\alpha_1 + \alpha_3}, \tag{8a}$$

$$\omega_2 = \left[\frac{1}{2}\left(2\alpha_1 + \alpha_2 + \Omega_{\text{conf}}^2\right) + \frac{1}{2}\sqrt{\left(\Omega_{\text{conf}}^2 - \alpha_2\right)^2 - 4\sigma_x^2}\right]^{1/2}, \tag{8b}$$

$$\omega_3 = \left[\frac{1}{2}\left(2\alpha_1 + \alpha_2 + \Omega_{\text{conf}}^2\right) - \frac{1}{2}\sqrt{\left(\Omega_{\text{conf}}^2 - \alpha_2\right)^2 - 4\sigma_x^2}\right]^{1/2}. \tag{8c}$$

For $(\Omega_{\text{conf}}^2 - \alpha_2)^2 - 4\sigma_x^2 < 0$, the imaginary part of the frequency is not zero and the instability will start. Without term $-4\sigma_x^2$ (depends on wake-charge $\tilde{q}$) in the above expression, instability will not occur. Note, for large Ω_{conf}^2, again there is no chance for resonance and the imaginary part of the frequency goes to zero. The limit of the confinement frequency comes from the following inequality:

$$\begin{aligned}\Omega_{\text{conf}}^2 < (1 - \tilde{q})\exp(-\kappa)(8 + 8\kappa + 4\kappa^2)\sin^2(ka/2) + 4\tilde{q}\tilde{\delta}[16\exp(-\sqrt{3}\kappa/2) \\ (4\sqrt{3} + 6\kappa + \sqrt{3}\kappa^2)\sin(ka/2) + 9\exp(-\kappa)(3 + 3\kappa + \kappa^2)\sin(ka)]/9.\end{aligned} \tag{9}$$

https://doi.org/10.1017/S0022377813001220 Published online by Cambridge University Press

In the coupling region, the real and imaginary parts of the frequency for $\tilde{q} \neq 0$ are

$$\omega = \omega_2 = \omega_3 = \left[\frac{1}{2}\left(2\alpha_1 + \alpha_2 + \Omega_{\text{conf}}^2\right)\right]^{1/2}, \tag{10a}$$

$$\omega_i = \frac{1}{4\omega}\left[4\sigma_x^2 - \left(\Omega_{\text{conf}}^2 - \alpha_2\right)^2\right]^{1/2}. \tag{10b}$$

When a wave propagates in (1,1,0) direction ($k_x = k_y = k/\sqrt{2}$) of the bcc crystal, the dispersion relation of modes reduces to

$$\omega_1 = \sqrt{\alpha_1 + \alpha_2 - \gamma}, \tag{11a}$$

$$\omega_2 = \left[\frac{1}{2}\left(2\alpha_1 + \alpha_2 + \gamma + \Omega_{\text{conf}}^2\right) + \frac{1}{2}\sqrt{\Omega_{\text{conf}}^4 - 2(\alpha_2 + \gamma)\Omega_{\text{conf}}^2 + (\alpha_2 + \gamma)^2 - 8\sigma_x^2}\right]^{1/2}, \tag{11b}$$

$$\omega_3 = \left[\frac{1}{2}\left(2\alpha_1 + \alpha_2 + \gamma + \Omega_{\text{conf}}^2\right) - \frac{1}{2}\sqrt{\Omega_{\text{conf}}^4 - 2(\alpha_2 + \gamma)\Omega_{\text{conf}}^2 + (\alpha_2 + \gamma)^2 - 8\sigma_x^2}\right]^{1/2}. \tag{11c}$$

For

$$\Omega_{\text{conf}}^4 - 2(\alpha_2 + \gamma)\Omega_{\text{conf}}^2 + (\alpha_2 + \gamma)^2 - 8\sigma_x^2 < 0, \tag{12a}$$

or

$$\alpha_2 + \gamma - 2\sqrt{2}\sigma_x < \Omega_{\text{conf}}^2 < \alpha_2 + \gamma + 2\sqrt{2}\sigma_x, \tag{12b}$$

the imaginary part of the frequency is not zero and the instability will start. In the coupling region, the real and imaginary parts of the frequency are

$$\omega = \omega_2 = \omega_3 = \left[\frac{1}{2}\left(2\alpha_1 + \alpha_2 + \gamma + \Omega_{\text{conf}}^2\right)\right]^{1/2}, \tag{13a}$$

$$\omega_i = \frac{1}{4\omega}\left[-\Omega_{\text{conf}}^4 + 2(\alpha_2 + \gamma)\Omega_{\text{conf}}^2 - (\alpha_2 + \gamma)^2 + 8\sigma_x^2\right]^{1/2}. \tag{13b}$$

Figure 2(a) shows the normalized longitudinal and transverse in-plane (horizontal) and the out-of-plane (vertical) dispersion relations of the wave propagating in the special case in which it propagates in (1,0,0) direction for the bcc configuration and the normalized confinement frequency $\Omega_{\text{Conf}} = 2.5$. From relations in (5), we conclude that all dispersion elements characterizing the dust-lattice modes have a common factor $(1-\tilde{q})$, i.e. if we divide all frequencies by $\sqrt{1-\tilde{q}}$, the new normalized frequencies are not affected by $\tilde{q}$. The coupling between the modes is determined by the product $\tilde{q}\tilde{\delta}$. The analysis shows that the value of $\tilde{q}\tilde{\delta}$ and the confinement frequency can affect coupling and the width of the hybridized zone of the dispersion relation. The imaginary part of (4) shows that the hybrid modes are always unstable. The imaginary part of the frequency is plotted for $\nu = 0$. For $\nu \neq 0$, all parts of frequencies have a little imaginary part and damping. By decreasing the confinement frequency, the coupling between the longitudinal in-plane (horizontal) and the out-of-plane (vertical) modes trigger at $\Omega_{\text{conf}} = 2.654$. The region of instability in the

https://doi.org/10.1017/S0022377813001220 Published online by Cambridge University Press

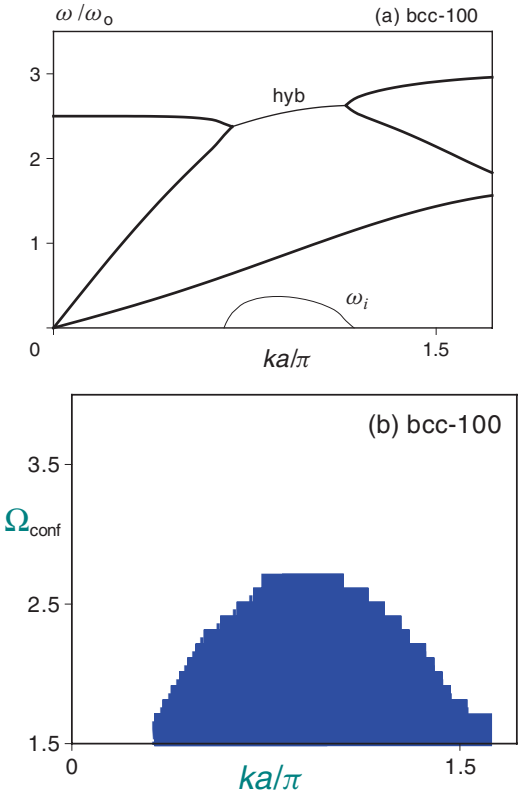


FIGURE 2. (Colour online) (a) Real and imaginary parts of normalized frequency propagated in (1,0,0) direction as a function of normalized wavenumber for $\Omega_{\text{conf}} = 2.5$ in the bcc dust lattice. (b) The instability area for variable Ω_{conf} and the normalized wavenumber ka/π. Parameters are $\kappa = 1.2$, $q/Q = -0.3$, and $\delta/a = 0.3$.

$(\Omega_{\text{conf}},\ ka/\pi)$ plane is depicted in Fig. 2(b). For smaller confinement frequency the larger intervals of wavenumbers are in instability area. Parameters in Fig. 2 are $\tilde{q} = 0.3$, $a/\lambda_D = 1.2$, and $\tilde{\delta} = 0.3$. Figures 3(a) and (b) are plotted for the waves which propagate in (1,1,0) direction. The coupling and instability starts at $\Omega_{\text{conf}} = 3.253$, which is greater than relative to (1,0,0) direction for the same physical parameters. In Fig. 3(b) there two distinct regions of instability for small confinement frequency. i.e. some part of the wavenumber is in stable region.

2.2. *Dispersion relations of the fcc configuration*

The matrix elements of the fcc configuration are:

$$\alpha_1 = (1-\tilde{q})\,\Omega_1 \left[\sin^2\left(\frac{k_x + k_y}{4}a\right) + \sin^2\left(\frac{k_x - k_y}{4}a\right)\right], \tag{14a}$$

$$\alpha_2 = (1-\tilde{q}) \left[2\Omega_1 \sin^2\left(\frac{k_x}{4}a\right) + \Omega_3 \sin^2\left(\frac{k_x}{2}a\right) - \Omega_2 \sin^2\left(\frac{k_y}{4}a\right)\right], \tag{14b}$$

$$\alpha_3 = (1-\tilde{q}) \left[2\Omega_1 \sin^2\left(\frac{k_y}{4}a\right) + \Omega_3 \sin^2\left(\frac{k_y}{2}a\right) - \Omega_2 \sin^2\left(\frac{k_x}{4}a\right)\right], \tag{14c}$$

https://doi.org/10.1017/S0022377813001220 Published online by Cambridge University Press

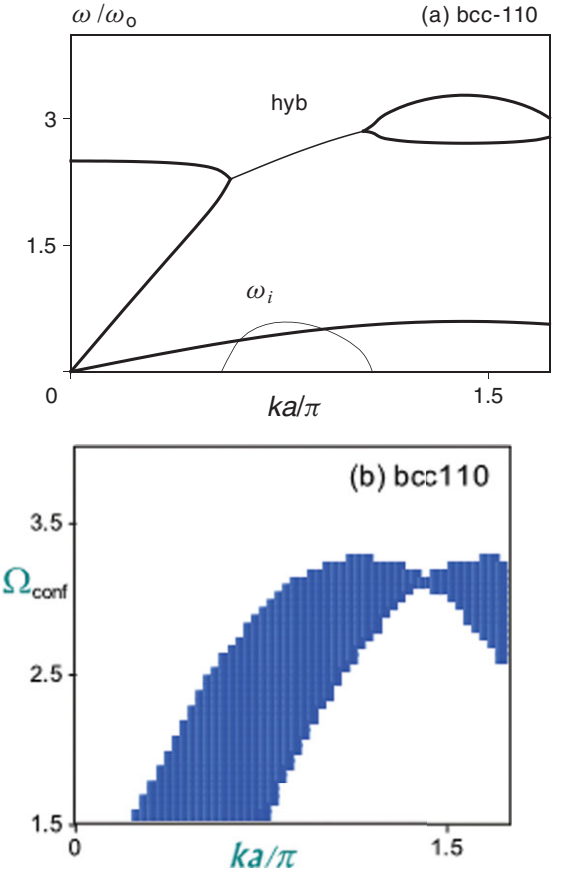


FIGURE 3. (Colour online) (a) Real and imaginary parts of normalized frequency propagated in (1,1,0) direction as a function of normalized wavenumber for $\Omega_{\rm conf} = 2.5$ in the bcc dust lattice. (b) The instability area for variable $\Omega_{\rm conf}$ and the normalized wavenumber ka/π. Parameters are $\kappa = 1.2$, $q/Q = -0.3$, and $\delta/a = 0.3$.

$$\gamma = (1-\tilde{q})\,(\Omega_1 + 0.5\Omega_2)\left[\sin^2\left(\frac{k_x+k_y}{4}a\right) - \sin^2\left(\frac{k_x-k_y}{4}a\right)\right], \tag{14d}$$

$$\sigma_x = \tilde{q}\tilde{\delta}(\Omega_1 + 0.5\Omega_2)\left[\sin\left(\frac{k_x+k_y}{2}a\right) + \sin\left(\frac{k_x-k_y}{2}a\right) + 2\sin\left(\frac{k_x}{2}a\right)\right] + \tilde{q}\tilde{\delta}\Omega_4 \sin(k_x a), \tag{14e}$$

$$\sigma_y = \tilde{q}\tilde{\delta}(\Omega_1 + 0.5\Omega_2)\left[\sin\left(\frac{k_x+k_y}{2}a\right) - \sin\left(\frac{k_x-k_y}{2}a\right) + 2\sin\left(\frac{k_y}{2}a\right)\right] + \tilde{q}\tilde{\delta}\Omega_4 \sin(k_y a), \tag{14f}$$

$$\Omega_1 = (4\sqrt{2} + 4\kappa + 2\sqrt{2}\kappa^2)\exp(-\sqrt{2}\kappa/2), \tag{14g}$$

https://doi.org/10.1017/S0022377813001220 Published online by Cambridge University Press

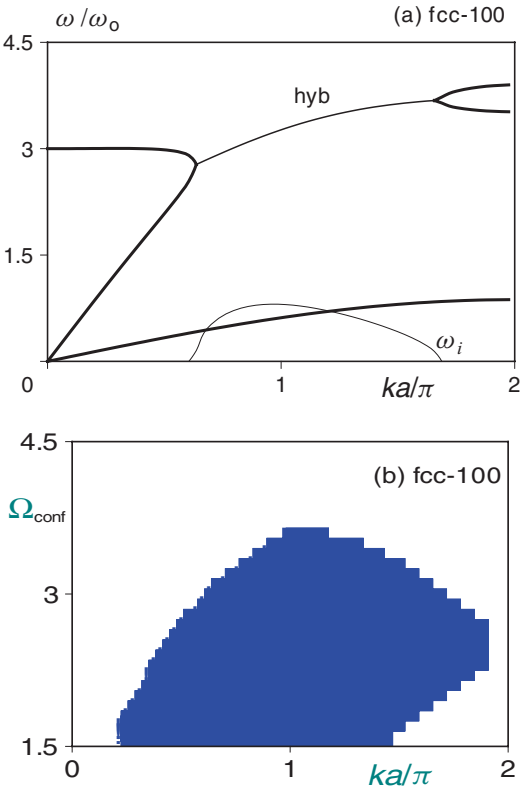


FIGURE 4. (Colour online) (a) Real and imaginary parts of normalized frequency propagated in (1,0,0) direction as a function of normalized wavenumber for $\Omega_{\text{conf}} = 3$ in the fcc dust lattice. (b) The instability area for variable Ω_{conf} and the normalized wavenumber ka/π. Parameters are $\kappa = 2.5$, $q/Q = -0.3$, and $\delta/a = 0.3$.

$$\Omega_2 = 16(\sqrt{2} + \kappa)\exp(-\sqrt{2}\kappa/2), \tag{14h}$$

$$\Omega_3 = 4(2 + 2\kappa + \kappa^2)\exp(-\kappa), \tag{14i}$$

$$\Omega_4 = (6 + 6\kappa + 2\kappa^2)\exp(-\kappa). \tag{14j}$$

The same as in bcc, the coupling can only be triggered when the confinement frequency Ω_{Conf} is below a critical value, which corresponds to the junction between the modes.

In a special case, when the wave propagates in (1,0,0) direction ($k_x = k, k_y = 0$), the dispersion relation of modes is governed by (8) and (10). Note, relations are the same as in the bcc configuration, but the coefficients are not the same. The limit of the confinement frequency comes from following inequality:

$$\begin{aligned}\Omega_{\text{conf}}^2 < {} & 4(1-\tilde{q})[\exp(-\kappa)(2 + 2\kappa + \kappa^2)\sin^2(ka/2) \\ & + \exp(-\kappa/\sqrt{2})(2\sqrt{2} + 2\kappa + \sqrt{2}\kappa^2)\sin^2(ka/4)] \\ & + 4\tilde{q}\tilde{\delta}[\exp(-\kappa/\sqrt{2})(10\sqrt{2} + 10\kappa + \sqrt{2}\kappa^2)\sin(ka/2) \\ & + \exp(-\kappa)(3 + 3\kappa + \kappa^2)\sin(ka)].\end{aligned} \tag{15}$$

https://doi.org/10.1017/S0022377813001220 Published online by Cambridge University Press

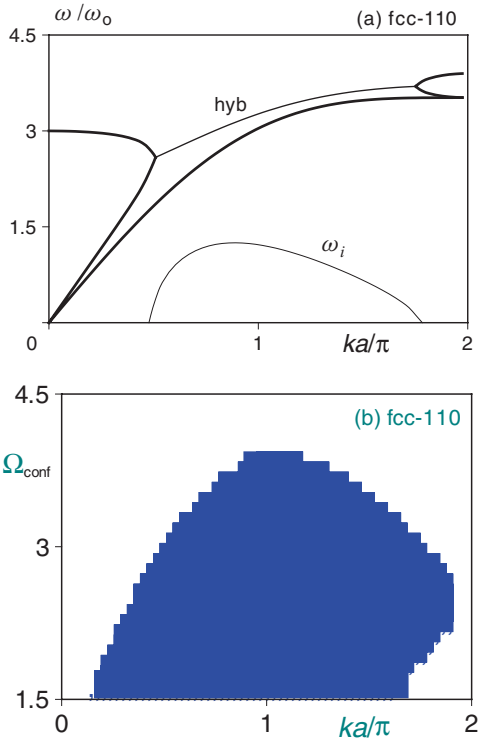


FIGURE 5. (Colour online) (a) Real and imaginary parts of normalized frequency propagated in (1,1,0) direction as a function of normalized wavenumber for $\Omega_{\rm conf} = 3$ in the fcc dust lattice. (b) The instability area for variable $\Omega_{\rm conf}$ and the normalized wavenumber ka/π. Parameters are $\kappa = 2.5$, $q/Q = -0.3$, and $\delta/a = 0.3$.

When the wave propagate in (1,1,0) direction ($k_x = k_y = k/\sqrt{2}$) of the fcc crystal, the dispersion relation of modes is the same as in (11)–(13).

Figures 4 and 5 show normalized modes in the special cases of (1,0,0) and (1,1,0) for the fcc configuration. The hybrid modes are unstable. The parameters in Figs. 4 and 5 are $\tilde{q} = 0.3$, $a/\lambda_D = 2.5$, and $\tilde{\delta} = 0.3$. The normalized confinement frequency in Figs. 4(a) and 5(a) is $\Omega_{\rm Conf} = 3$.

The same as in the bcc configuration, in the fcc configuration the instability will start for $\Omega_{\rm conf} < \Omega_{\rm cr}$. The critical values of the confinement frequency are $\Omega_{\rm cr} = 3.509$ and 3.834 for (1,0,0) and (1,1,0) directions respectively. The critical values of confinement frequencies in the fcc configuration are larger than that for the bcc configuration.

3. Conclusions

In summary, the longitudinal, transverse (horizontal), and optic-like (vertical) modes in the 3D dust-lattice configuration taking into account particle–wake interactions are found linearly. The wakefield was modeled using a simple but effective image charge method.

Interaction of dusts and wake-charges lead to mode coupling instability, which can cause crystal melting. Intersection of optical and longitudinal modes causes hybridization and triggers instability.

https://doi.org/10.1017/S0022377813001220 Published online by Cambridge University Press

The values for $\tilde{q}$ and $\tilde{\delta}$ in plasma bulk have been obtained by simulations. Values of parameters are related to discharge parameters such as pressure, temperature, fields, etc. In this paper, we have used $\tilde{q} = 0.3$, $\tilde{\delta} = 0.3$ (based on Schweigert et al. 1996). By changing $\tilde{q}$ and $\tilde{\delta}$, the width of the hybridized zone will change. The coupling between the modes is determined by the product $\tilde{q}\tilde{\delta}$, which is the dipole strength, and one can use dipolar interaction instead of the Yukawa form for particle–wake interaction. The instability (due to coupling between the out-of-plane mode and the longitudinal in-plane mode) starts for confinement frequency below its critical value. It is expected that under certain conditions, based on these result, bcc and fcc plasma crystals can be formed in experiments and crystals would melt by decreasing the confinement potential.

REFERENCES

Bonitz, M., Henning, C. and Block, D. 2010 *Rep. Prog. Phys.* **73**, 066501.
Chu, J. H. and Lin, I. 1994 *Phys. Rev. Lett.* **72**, 4009. doi:10.1103/PhysRevLett.72.4009.
Farokhi, B. and Hameditabar, A. 2012 *Chinese Phys. Lett.* **29**, 025204.
Hamaguchi, S., Farouki, R. T. and Dubin, D. H. E. 1997a *Phys. Rev. E* **56**, 4671.
Hamaguchi, S., Farouki, R. T. and Dubin, D. H. E. 1997b *Phys. Rev. E* **56**, 46.
Hayashi, Y. 1999 *Phys. Rev. Lett.* **83**, 4764. doi:10.1103/PhysRevLett.83.4764.
Ignatov, A. M. 2003 *Plasma Phys. Rep.* **29**, 296.
Ikezi, H. 1986 *Phys. Fluids.* **29**, 1764.
Ivlev, A. V. and Morfill, G. 2001 *Phys. Rev. E* **63**, 026412.
Klumov, B. A. and Morfill, G. E. 2008 *J. Exp. Theor. Phys.* **107**, 908.
Klumov, B. A. and Morfill, G. E. 2009 *J. Exp. Theor. Phys.* **90**, 489.
Morfill, G. E. et.al. 1997 *Advances in Dusty Plasma Physics.* Singapore: World Scientific, 99 pp.
Pieper, J. B., Goree, J. and Quinn, R. A. 1996 *J. Vac. Sci. Technol. A* **14**, 519. doi:10.1116/1.580118.
Schweigert, V. A., Schweigert, I. V., Melzer, A., Homann, A. and Piel, A. 1996 *Phys. Rev. E* **54**, 4155.
Thomas, H., Morfill, G. E., Demmel, V., Goree, J., Feuerbacher, B. and Mohlmann, D. 1994 *Phys. Rev. Lett.* **73**, 652.
Vaulina, O., Khrapak, S. and Morfill, G. E. 2002 *Phys. Rev. E* **66**, 016404.
Wang, X. Y., Duan, W. S., Lin, M. M. and Wan, G. X. 2006 *Chaos Solitons Fractals* **30**, 909. doi:10.1016/j.chaos.2005.08.193.
Yang, X. F. and Wang, X. G. 2012 *Phys. Plasmas* **19**, 073704.
Yang, X. F., Wang, X. G. and Liu, Y. 2009 *Chinese Phys. B* **18**, 4938.
Zhdanov, S. K., Ivlev, A. V. and Morfill, G. E. 2009 *Phys. Plasmas* **16**, 083706.
Zuzic, M., Ivlev, A. V. and Goree, J. 2000 *Phys. Rev. Lett.* **85**, 4064.

https://doi.org/10.1017/S0022377813001220 Published online by Cambridge University Press